Title
MEASUREMENTS OF THE COSMIC MICROWAVE BACKGROUND RADIATION TEMPERATURE AT 90 GHZ

Authors
Bersanelli, M.
Witebsky, C.
Bensadoun, M.

Publication Date
1988-08-01

LBL-25673
Preprint

Lawrence Berkeley Laboratory
UNIVERSITY OF CALIFORNIA

Physics Division

Submitted to Astrophysical Journal

Measurements of the Cosmic Microwave Background Radiation Temperature at 90 GHz

M. Bersanelli, C. Witebsky, M. Bensadoun, G. De Amici,
A. Kogut, S.M. Levin, and G.F. Smoot

August 1988

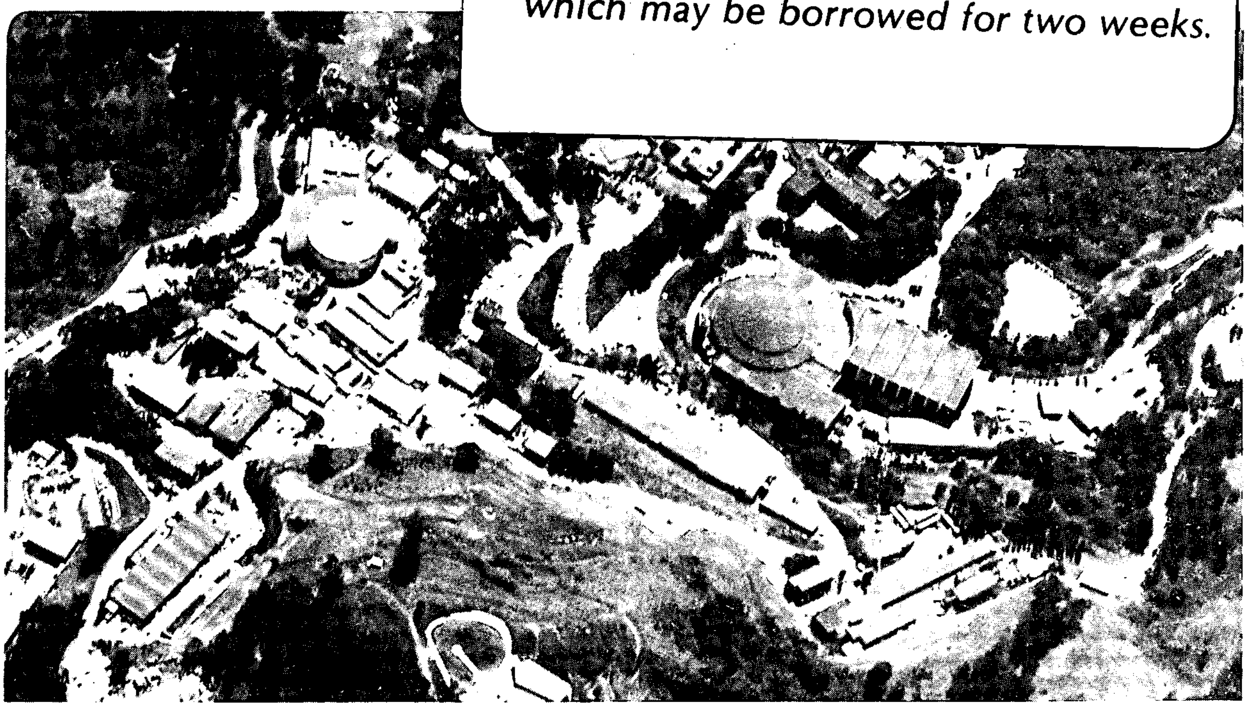

Prepared for the U.S. Department of Energy under Contract Number DE-AC03-76SF00098.

MEASUREMENTS OF THE COSMIC MICROWAVE BACKGROUND RADIATION TEMPERATURE AT 90 GHZ

Marco Bersanelli,[1] Chris Witebsky, Marc Bensadoun, Giovanni De Amici, Al Kogut, Steven M. Levin, and George F. Smoot

Space Sciences and Lawrence Berkeley Laboratory
University of California at Berkeley

ABSTRACT

We have measured the temperature of the cosmic microwave background radiation (CMBR) at 90 GHz (0.33 cm wavelength) in the summers of 1986 and 1987 using a Dicke-switched ground-based radiometer. These measurements are part of a larger effort to measure the CMBR spectrum in the Rayleigh-Jeans region (Smoot *et al.*), and represent an extension of the work by Witebsky *et al.* The weighted average for five years' observations gives a thermodynamic temperature of 2.60 ± 0.09 K at the 68% confidence level. This result is in agreement with measurements obtained by other methods at comparable frequencies (Peterson, Richards, and Timusk; Meyer and Jura; Crane *et al.*), in particular providing a useful comparison to the recent measurement by Matsumoto *et al.* at shorter wavelengths.

I. INTRODUCTION

Measurements of the cosmic microwave background radiation (CMBR) provide information on the early history of the universe. In principle any energy release occurring at a red shift less than about 10^6 is able to distort the spectrum from its initially planckian shape, the form of distortion depending on the time, amount and mechanism of the energy release (Danese and De Zotti 1977; Sunyaev and Zel'dovich 1970). Recent ground-based measurements (Smoot *et al.* 1987; Sironi *et al.* 1987) have greatly improved the accuracy in the Rayleigh-Jeans region of the CMBR spectrum at frequencies above 600 MHz. Interesting results have been obtained in the high frequency region of the spectrum, where the rocket-borne experiment by Matsumoto *et al.* (1988) seems to provide evidence for a spectral distortion at $\nu > 300$ GHz. Independent measurements at comparable frequencies represent therefore an important crosscheck for those results. Here we report the results of further ground-based measurements at 90 GHz, made in 1986 and 1987 in conjunction with CMBR temperature measurements at 1.5, 3.8, and 10 GHz.

II. INSTRUMENT AND CONCEPT OF THE EXPERIMENT

We perform these measurements with a Dicke-switched radiometer, a device whose output is proportional to the difference in the electromagnetic power per unit bandwidth

[1]Now at the Istituto di Fisica Cosmica--CNR, Milano, Italy

entering its two input ports. Feeding the input ports are two corrugated conical antennas pointing 60 degrees apart with a half power beam width (HPBW) of 7.5° and very good sidelobe suppression to minimize the effect of ground radiation (Janssen *et al.* 1979). A switch alternately connects one of the two antennas to the receiver at a switching frequency of 100 Hz. The signal is then downconverted to a double side bandwidth of 0.1 to 1.0 GHz, amplified, and rectified by a square-law detector diode. A lock-in amplifier produces an output signal proportional to the difference in power at the two input antennas. The signal is averaged with a 2-second integration time, digitized by a 16-bit analog/digital converter (ADC), and recorded on digital cassette tape and floppy disk. Table I lists the main characteristics of the instrument, which is described in greater detail by Witebsky *et al.* (1986).

The signal is measured in units of antenna temperature T_A, defined as:

$$T_A = \frac{P}{kB} = \frac{T_\nu}{\exp(T_\nu / T) - 1} \qquad (1)$$

where $T_\nu = h\nu/k$ (= 4.32 K at 90 GHz), h is Planck's constant, k is Boltzmann's constant, P is power, and B is the bandwidth of the radiometer; T is the physical temperature of a blackbody field completely filling the antenna beam. If the antennas view two blackbody targets at temperatures T_1 and T_2 the measured signal is:

$$S = \frac{1}{G}[(T_{A,1} - T_{A,2}) + T_{off}] \qquad (2)$$

where G is the gain calibration coefficient and T_{off} is the radiometer's offset. We measure the antenna temperature of the zenith sky, $T_{A,zen}$, by comparing it to the known signal from a cryogenic blackbody calibrator at liquid helium (LHe) temperature. The detected signal from the zenith is the sum of the antenna temperature of the CMBR, $T_{A,CMBR}$, plus other contributions, each of which is evaluated and subtracted:

$$T_{A,CMBR} = T_{A,zen} - T_{A,atm} - T_{A,gal} - T_{A,gr} \qquad (3)$$

Here $T_{A,atm}$, $T_{A,gal}$, and $T_{A,gr}$ are the antenna temperatures of the signals due to the emission from, respectively, the atmosphere, the galaxy, and the ground. The atmospheric term includes a term for attenuation of galactic and cosmic radiation by the atmosphere.

At 90 GHz the contribution from the atmosphere constitutes more than 90% of the total zenith temperature. To minimize $T_{A,atm}$ we perform the measurement from a dry (< 5 mm H_2O), high altitude (3800 m) site: the White Mountain Research Station, on Mount Barcroft, California. The choice of this site reduces the atmospheric contribution by at least a factor of 3 compared to measurements at sea level in Berkeley. The atmospheric emission in this spectral region is almost entirely due to pressure-broadened line emission from O_2 and H_2O molecules. The variability of the column density of water vapor can cause $T_{A,atm}$ to change significantly in a time scale of a few minutes. Hence we plan the observing sequence in order to obtain several independent and almost simultaneous measurements of $T_{A,zen}$ and $T_{A,atm}$.

Table II summarizes the important features of the steps in each observing cycle. All the measurements are symmetric with respect to the two antennas in order to cancel the radiometer's offset and minimize pointing errors. Steps 1 and 3 measure $T_{A,zen}$ (see fig. 1a); steps 2 and 4 provide an independent measurement of G for each observation (fig. 1b). We measure $T_{A,atm}$ by tilting the antennas to different zenith angles (steps 5 to 9; see fig. 1c) and fitting the data to an atmospheric model to yield two independent evaluations of $T_{A,atm}$ for each observing cycle.

III. RADIOMETER TESTING

The radiometer configuration has remained essentially unchanged since the 1983 observations. A defective detector diode caused a large statistical spread in the data of 1984 (110 mK); this component was replaced before the 1986 measurements, resulting in a much more stable output signal. In 1987 the radiometer was modified to allow the operator to change the gain of the lock-in amplifier during observations. In this way we could perform some high-gain measurements of the atmosphere to check on possible ADC non-linearities or ground loops (the ADC is located downstream of the lock-in amplifier). For calibrations the gain is reset to the lower range to avoid saturation. As a cross-check on the data-recording system, the lock-in output voltages during several 1987 atmospheric measurements were recorded by hand as well. The radiometer performance has been intensively tested before and after the observations, both in Berkeley and at the White Mountain observation site. Tests show that the system noise fluctuation (89 ± 1 mK for an integration time $t = 2$ seconds) decreased according to $t^{-1/2}$ (as expected for gaussian fluctuations) for periods much larger than the 192 s required to complete an observation. A number of tests were performed to check possible changes in the radiometer's offset when the instrument was tilted to different angles. In these tests both antennas viewed Eccosorb targets cooled to liquid nitrogen (LN) temperature while the radiometer was repeatedly rotated between two or more symmetric positions (Witebsky *et al.* 1986). The results show that all corrections and uncertainties are ≤ 10 mK (detailed results are listed in Table III). We tested also for sensitivity of the radiometer's offset to external magnetic fields: the effect of the earth's magnetic field is less than 2 mK.

We also performed radiometric measurements of the atmospheric temperature (atmospheric scans) as a general test of the radiometer's performance and to provide useful data for the evaluation of atmospheric emission and stability. These complemented similar measurements of the CMBR and atmosphere at lower frequencies (Levin *et al.* 1988; De Amici *et al.* 1988; Kogut *et al.* 1988). The observing procedure consisted of steps 5 through 9 of Table II, preceded and followed by two symmetric calibration measurements. The ambient temperature target and the zenith sky (typically about 10 K) were used as calibration loads; G was then calculated iteratively.

IV. OBSERVATIONS AND DATA ANALYSIS

The observations are made at night to avoid the contribution and thermal effects of the sun; also, the atmosphere is usually more stable and dry during the night-time. Data were taken with LHe in the cold load on the nights of 1986 August 8 and 9 and 1987 September 15 (U.T.). Observations with LN in the cold load were made on the nights of 1986 August 6 and 7 and 1987 September 11 (U.T.), as a general test of the equipment and procedure. The data are selected as follows: data points taken while the radiometer was moving from one position to the next are identified and rejected; the data corresponding to each step are then averaged over the remainder of the 16- or 32-second interval; the averages are plotted to identify errors in the observing routine, evidence of clouds in the antenna beam, or apparent radiometer problems. This analysis shows that some 30% of the data from 1986 are of poor quality, due to improper calibration measurements and atmospheric instability. These data values are eliminated from further analysis. These deletions alter the final result by less than 10 mK.

Each observing cycle gives an independent measurement of G, $T_{A,zen}$ and $T_{A,atm}$. From steps 2 and 4 we find the calibration coefficient:

$$G = 2\frac{T_{amb} - T_{load}}{S_{amb/load} - S_{load/amb}} \tag{4}$$

where T_{amb} and T_{load} are the antenna temperatures of the ambient and cryogenic targets, and the terms $S_{amb/load}$ and $S_{load/amb}$ are the radiometer signals when the two antennas view the ambient and cold loads (see Table II). In this relation, as well as in the next two, we remove the radiometer's offset by taking the difference of symmetric measurements.

To calculate $T_{A,zen}$ we used steps 1 and 3 and the relation:

$$T_{A,zen} = \frac{G}{2}(S_{zen/load} - S_{load/zen}) - \frac{\delta T_{off}}{2} + T_{load} - T_{refl} \tag{5}$$

where δT_{off} is the offset change discussed in section III and T_{refl} accounts for the emission from the mirrors which reflect the zenith radiation into the antennas (see fig. 1). Each cycle measures $T_{A,atm}$ twice: steps 5 and 9 give an evaluation based on the atmospheric signal at zenith angles of $\pm 50°$ and $\mp 10°$ ($T_{A,atm\ 50/10}$); steps 6 and 8 give an evaluation for $\pm 40°$ and $\mp 20°$ angles ($T_{A,atm\ 40/20}$). The value of $T_{A,atm}$ is the average of the two measurements. We evaluated $T_{A,atm\ Z_1/Z_2}$ from measurements at zenith angles Z_1 and Z_2 by fitting difference terms of the type

$$\Delta T_{A,atm\ Z_1/Z_2} = \frac{1}{2}(S_{Z_1/Z_2} - S_{Z_2/Z_1}) - \frac{\delta T_{off\ Z_1/Z_2}}{2} - T_{A,gr\ Z_1/Z_2} \tag{6}$$

into an atmospheric model. The model, described in detail by Witebsky *et al.* (1986) assumes $T_{atm}(Z)$ to have a functional form that varies approximately as sec (Z) but also includes corrections for atmospheric self-absorption (≈ 0.3 K near the zenith), the effect of the finite width of the antenna beam (≈ 0.1 K), and minor effects such as variation of the atmospheric temperature profile (< 10 mK) and curvature of the atmospheric layer (< 5 mK). Table IV lists the results of all the data processed in the described way for each observation run, together with their uncertainties (68% confidence level). It also includes the corresponding CMBR antenna temperatures, obtained using eq. (3), and their uncertainties.

An analysis of all the 1987 atmospheric data recorded by the data-logging system shows that the quantity

$$\delta T_{50/40} = T_{A,atm\ 50/10} - T_{A,atm\ 40/20}$$

is systematically positive. A weighted average of all 78 scans gives $\delta T_{50/40} = 0.102 \pm 0.011$ K. We have also analyzed the atmospheric measurements using the data from individual scan positions, combined with the corresponding 30° South/30° North data (step 7 in Table II) to eliminate the offset. Although this procedure does not provide very precise estimates, it is clear that the evaluations using the 40° South/20° North measurement (step 6) are about 0.2 K lower than the other three. We have collected an additional 102 atmospheric measurements using a digital volt-meter (DVM) to measure the time-averaged lock-in output and recording the numbers by hand. From these measurements we derive

$\delta T_{50/40}$ = -0.024 ± 0.013 K (68% c. l.), in sharp contrast to the +0.102 K value derived above.

Fifteen atmospheric scans have been recorded both by hand and by the data-logging system. Readings digitized independently by both the ADC and the DVM show a general agreement between the respective 50/10 evaluations (the mean difference between measurements is -0.040 ± 0.009 K), but a disagreement in the 40/20 evaluations (a mean difference of -0.206 ± 0.035 K, the temperature measured with the DVM being higher). This evidence suggests a subtle malfunction of the data-recording system, possibly a localized nonlinearity in the ADC in the range corresponding to the radiometer output voltage at 40 South/20 North. Data values recorded at other positions do not show any similar effects. We have therefore chosen to use only $T_{A,atm\ 50/10}$ in computing $T_{A,CMBR}$ from the 1987 data. Although there is no evidence of this problem in the 1986 data, we have chosen to add half the average difference between the two evaluations (38 mK) as a safe limit on systematic errors.

V. SYSTEMATIC UNCERTAINTIES

Table III lists the estimated systematic errors in the 1986 and 1987 observations (for a detailed analysis of each term see Witebsky *et al.* 1986). Pointing errors are slightly larger in 1986 because of the larger value of $T_{A,atm}$ in that year. The pointing angles are carefully measured before and after the observation with a precision clinometer, and they are repeatable at 2' or better; this results in less than 20 mK uncertainty in $T_{A,CMBR}$.

Better limits in 1987 on the fractional gain drift $\delta G/G$ and on possible saturation effects (derived from a combination of the calibration measurements with LN and with LHe) reduce the gain-related errors in $T_{A,CMBR}$ to ± 4 mK.

The cold load (Smoot *et al.* 1983) was at a pressure of 489 ± 2 mm Hg, corresponding to a LHe boiling temperature of 3.782 ± 0.004 K. We tested for reflection effects due to the two polyethylene windows at the mouth of the dewar and found a total upper limit of 35 ± 35 mK for both coherent and incoherent effects. Accounting also for the emission from the inside walls and from the windows themselves, the total antenna temperature of the cold load was $T_{A,load}$ = 2.087 ± 0.037 K.

VI. RESULTS AND INTERPRETATION

Table V presents the results of all our CMBR measurements at 90 GHz. With the exception of the 1984 result, the uncertainty in each of the measurements is dominated by systematic errors. The much larger error in 1982 is due to a pointing uncertainty related to a different radiometer configuration used in that year (Witebsky *et al.* 1986). To compute a weighted average of these five results, we weight each $T_{A,CMBR}$ with the corresponding statistical uncertainty summed in quadrature with those systematic errors which are nearly independent from year to year. Other systematic effects (those due to ground radiation, atmospheric modeling, calibration load, and emission from the reflectors) are likely to be constant for all the measurements, and can not be used as weighting factors; to compute the total uncertainty we add in quadrature the average of these effects (58 mK) with the statistical sigma resulting from the weighted average (42 mK). Then we convert the final antenna temperature (1.008 ± 0.071 K) into thermodynamic temperature and obtain:

$$T_{CMBR} = 2.60 \pm 0.09 \text{ K}. \qquad (7)$$

This result is in good agreement with previous heterodyne measurements in this spectral region (fig. 2), which have a weighted value of $T_{CMBR} = 2.55 \pm 0.10$ K (Boynton *et al.* 1968; Kisliakov *et al.* 1971; Millea *et al.* 1971; Boynton and Stokes 1974). It is also in statistical agreement with the CMBR temperatures obtained by Meyer and Jura (1985) and by Crane *et al.* (1986) from spectroscopic measurements of CN interstellar molecules at 113.6 GHz, and with the balloon-borne bolometric measurements by Peterson, Richards and Timusk (1985) at 85.5 GHz. A weighted average of our result with all previous results between 85 and 115 GHz gives $T_{CMBR} = 2.70 \pm 0.03$ K. A fit to all the CMBR temperatures measured at 600 MHz $\leq \nu \leq$ 300 GHz gives $T_{CMBR} = 2.74 \pm 0.02$ K. A detailed analysis of all recent CMBR measurements is found in Smoot *et al.* (1988).

We wish to thank many people for their help during this experiment: J. Aymon, H. Dougherty, J. Gates, J. Gibson, P. Lubin, F. Mitschang, A. Meuti, G. Sironi, and the staff and crew of the White Mountain Research Station. This work was supported in part by National Science Foundation grant AST - 8406187, by Department of Energy under contract DE-AC03-76SF00098, by CNR fellowships n. 203.2.13 and 203.2.15, by ISTRA (Istituto Studi per la Transizione) of Milano and by Fondazione Ing. A. Gini of Padova, Italy.

REFERENCES

Boynton, P. E., and Stokes, R. A. 1974, *Nature*, **247**, 528.

Boynton, P. E., Stokes, R. A., and Wilkinson, D. T. 1968, *Phys. Rev. Letters*, **21**, 462.

Crane, P., Heygi, D. J., Mandolesi, N., and Danks, A. C. 1968, *Ap. J.*, **309**, 822.

Danese, L. and De Zotti, G. 1977, *Riv. Nuovo Cimento*, **7**, 277.

De Amici, G., Smoot, G., Aymon, J., Bersanelli, M., Kogut, A., Levin, S., and Witebsky, C. 1988, *Ap. J.*, **329**, 556.

Janssen, M. A., Bednarczyk, S. M., Gulkis, S., Marlin, H. W., and Smoot, G. 1979, *IEEE Trans.*, **AP-27**, 551.

Kislyakov, A. G., Chernyshev, V. I., Lebskii, Yu. V., Mal'tsev, V. A., and Serov, N. V. 1971, *Astr. Zh.*, **48**, 39 (1971, *Soviet Astr.*, **15**, 29).

Kogut, A., *et al.* 1988, *Ap. J.* , **325**, 1.

Levin, S. M., Witebsky, C., Bensadoun, M., Bersanelli, M., De Amici, G., Kogut, A., and Smoot, G. 1988, *Ap J.*, in press.

Matsumoto, T., Hayakawa, S., Matsuo, H., Murakami, H., Sato, S., Lange, A. E., and Richards, P. L. 1988, *Ap. J.*, **329**, 567.

Meyer, D. M., and Jura, M. 1985, *Ap. J.* , **297**, 119.

Millea, M. F., *et al.* 1971, *Phys. Rev. Letters*, **26**, 919.

Peterson, J. B., Richards, P. L. and Timusk, T. 1985, *Phys. Rev. Letters*, **55**, 332.

Sironi, G., Bersanelli, M., Bonelli, G., Conti, G., Marcellino, G., Limon, M., and Reif, K. 1987, *13th Texas Symposium on Relativistic Astrophysics*, ed. M. P. Ulmer (Singapore: World Scientific Publishing), p. 245.

Smoot, G. F., *et al.* 1983, *Phys. Rev. Letters*, **51**, 1099.

Smoot, G. F., Bensadoun, M., Bersanelli, M., De Amici, G., Kogut, A., Levin, S. M., and Witebsky, C. 1987, *Ap. J. Letters*, **317**, L45.

Smoot, G. F., Levin, S. M., Witebsky, C., De Amici, G., Rephaeli, Y. 1988, *Ap. J.*, **331**, in press.

Sunyaev, R. A. and Zel'dovich, Y. B. 1970, *Ap. Space Sci.*, **7**, 20.

Witebsky, C. Smoot, G., De Amici, G., and Friedman, S. D. 1986, *Ap. J.*, **310**, 145.

TABLE I
GENERAL PROPERTIES OF THE 90 GHz SYSTEM

Receiver	differential (Dicke) type
Frequency	90.0 GHz
Bandwidth (DSB)	2.0 GHz
IF Passband	0.1-1.0 GHz
Integration time	2 s
Noise temperature	1530 ± 20 K
Sensitivity	126 ± 2 mK $Hz^{-1/2}$
Antennas HPBW	7.5°
Gain scales	37 K/V, 740 mK/V
Full range	± 10 V
Calibrator	LHe cold load
Observing site	White Mountain Research Station (lat. +38°, el. 3800 m)

TABLE II
OBSERVATION PROCEDURE

Step	South Antenna Load	North Antenna Load	Output	Time (sec)
1.	Zenith sky	LHe target	$S_{zen/load}$	32
2.	Ambient target	LHe target	$S_{amb/load}$	16
3.	LHe target	Zenith sky	$S_{load/zen}$	32
4.	LHe target	Ambient target	$S_{load/amb}$	16
5.	Southern Sky at Z=50°	Northern Sky at Z=10°	$S_{50/10}$	32
6.	Southern Sky at Z=40°	Northern Sky at Z=20°	$S_{40/20}$	16
7.	Southern Sky at Z=30°	Northern Sky at Z=30°	$S_{30/30}$	16
8.	Southern Sky at Z=20°	Northern Sky at Z=40°	$S_{20/40}$	16
9.	Southern Sky at Z=10°	Northern Sky at Z=50°	$S_{10/50}$	16

TABLE III
SYSTEMATIC ERRORS

Source of error	Value 1986	Value 1987	Error 1986	Error 1987	Error in $T_{A,CMBR}$ (mK) 1986	Error in $T_{A,CMBR}$ (mK) 1987
a) Gain						
Gain drift	35.806 K/V		0.05%	0.02%	8	3
Calibration load	to		0.65%	0.65%	9	9
Angular dependence	37.310 K/V		0.1%	0.1%	15	14
Nonlinearity			0.8%	0.2%	12	3
b) Zenith temperature						
Zenith offset	17 mK	16 mK	8 mK	12 mK	4	6
Ground radiation	12 mK	12 mK	15 mK	15 mK	15	15
Reflector emission	312 mK	312 mK	45 mK	45 mK	45	45
Cold load	2087.mK	2087 mK	37 mK	37 mK	37	37
c) Atmospheric temperature						
Ground radiation	0 mK	0 mK	$^{+15}_{-0}$ mK	$^{+15}_{-0}$ mK	$^{+30}_{-0}$	$^{+30}_{-0}$
40/20 offset	5 mK	10 mK	6 mK	3 mK	7	4
50/10 offset	12 mK	12 mK	5 mK	3 mK	3	6
Pointing:						
N/S cart tilt			30'	30'	11	9
Antenna misalignment			0.4'	0.4'	55	50
position uncertainty			2'	2'	20	18
Modeling			32 mK	26 mK	32	26
Atmospheric asymmetry			75 mK		38	
TOTAL					102	89

TABLE IV
RESULTS OF THE 1986 AND 1987 CMBR MEASUREMENTS

Date Time	Number of observations	G (K/V)	$T_{A,zen}$ (K)	$T_{40/20}$ (K)	$T_{50/10}$ (K)	$T_{A,CMBR}$(*) (K)
8/8/86 5:16-6:31	11	35.884 ±0.075	16.669 ±0.134	15.558 ±0.523	15.529 ±0.131	1.125 ±0.286
8/8/86 8:59-9:15	6	35.910 ±0.020	15.908 ±0.110	14.929 ±0.227	15.023 ±0.215	0.931 ±0.334
8/9/86 8:23-8:59	11	36.094 ±0.082	15.625 ±0.208	14.503 ±0.294	14.586 ±0.184	1.080 ±0.272
9/15/87 0:09-9:32	8	37.339 ±0.020	14.817 ±0.074	13.628 ±0.094	13.806 ±0.100	1.011 ±0.065

(*) - In the 1987 run only the atmospheric temperature measured at ± 50° and ±10° is used.

TABLE V
COMBINED RESULTS

Year	$T_{A,CMBR}$ (K)	Statistical error (K)	Systematic error (K)	T_{CMBR} (K)
1982	1.00 ± 0.57	0.034	0.570	$2.58^{+0.68}_{-0.79}$
1983	0.99 ± 0.09	0.016	0.090	2.57 ± 0.12
1984	0.96 ± 0.14	0.110	0.090	2.53 ± 0.18
1986	1.07 ± 0.11	0.054	0.102	2.68 ± 0.14
1987	1.01 ± 0.09	0.023	0.089	2.60 ± 0.11

FIGURE CAPTIONS

1 - The 90 GHz radiometer configuration: a. zenith sky measurements; b. calibration; c. atmospheric scan.
2 - Plot of recent CMBR measurements near 90 GHz.

MARC BENSADOUN, GIOVANNI DE AMICI, AL KOGUT, STEVEN M. LEVIN, GEORGE F. SMOOT, and CHRIS WITEBSKY: 50/232 Lawrence Berkeley Laboratory, University of California, Berkeley, CA 94720

MARCO BERSANELLI: Istituto di Fisica Cosmica, CNR, via Bassini 15, 20133 Milano, Italy

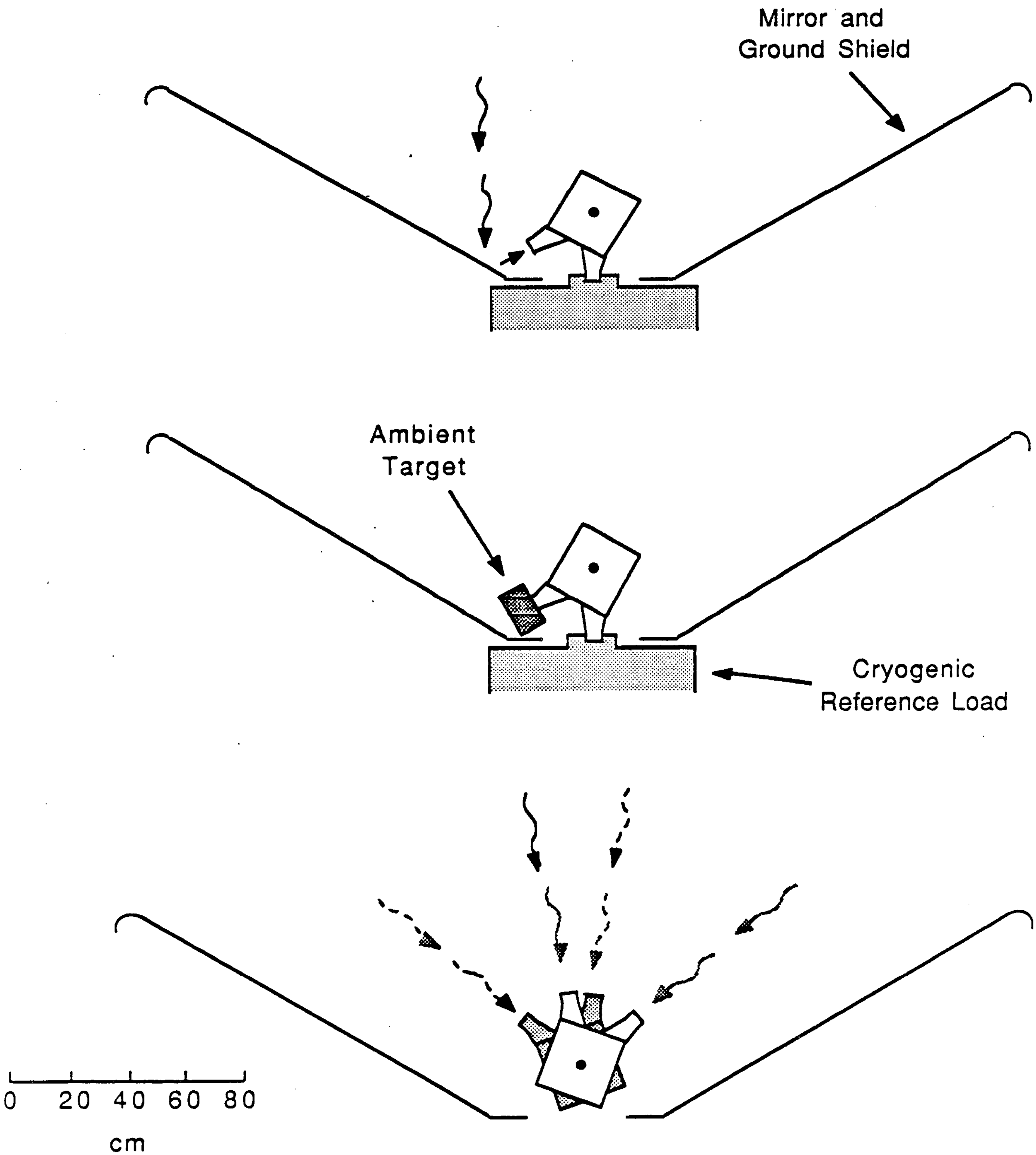
Mirror and
Ground Shield
Ambient
Target
Cryogenic
Reference Load
0 20 40 60 80
cm

Fig. 1

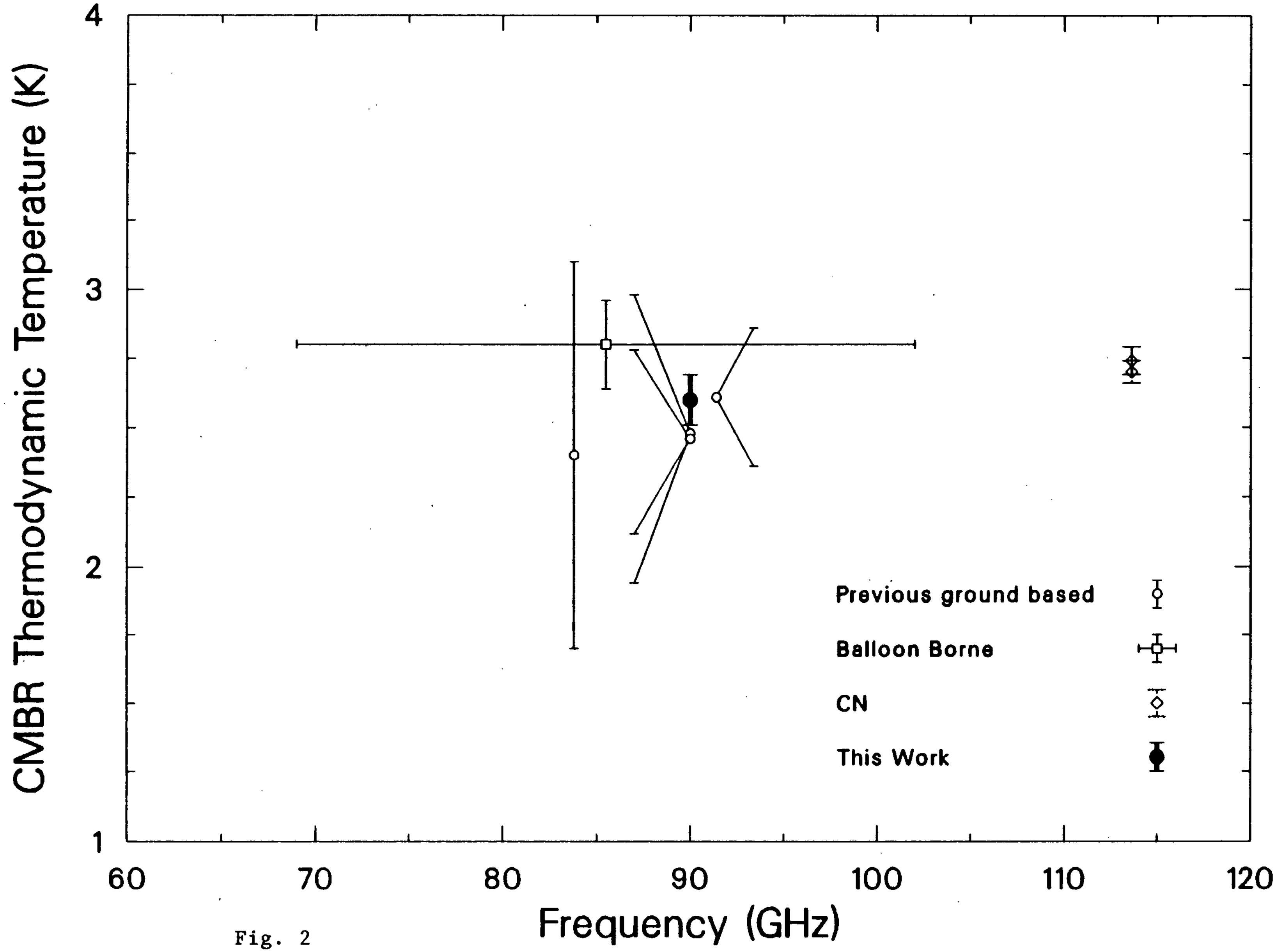
CMBR Thermodynamic Temperature (K)
4
3
2
1
60
70
80
90
100
110
120
Frequency (GHz)
Previous ground based
Balloon Borne
CN
This Work

Fig. 2

LAWRENCE BERKELEY LABORATORY
TECHNICAL INFORMATION DEPARTMENT
UNIVERSITY OF CALIFORNIA
BERKELEY, CALIFORNIA 94720